Ann. Acad. Rom. Sci.
Ser. Math. Appl.
ISSN 2066-6594 Vol. 17, No. 3/2025

NON-ISOTHERMAL FLOW OF A RAREFIED GAS IN 3D-DOMAINS*

Elvira Barbera† Claudia Fazio‡

Dedicated to Prof. Liliana Restuccia on the occasion of her 70th anniversary

DOI 10.56082/annalsarscimath.2025.3.55

Abstract

Stationary flow with heat transfer in a gas is investigated within Rational Extended Thermodynamics. A rarefied gas is considered in the gap between two confocal elliptical cylinders or non-coaxial circular ones. In both symmetries, internal and external cylinders are kept at two different constant temperatures and a flow in the axial direction is generated. Both Couette and Poiseuille problems are studied in these two symmetries. The solutions of the linearized field equations are determined and compared with the solutions of Classical Thermodynamic. Then, some non-linear effects are investigated. It is shown that the non-linear terms are able to describe some additional effects that are present in the Kinetic Theory but cannot be obtained within Classical Thermodynamics. In particular, non-vanishing stress tensor components and an axial heat flux are recovered in addition to the classical solutions.

Keywords: heat transfer, non-isothermal flow, rational extended thermodynamics, Grad theory.

MSC: 76P05, 80A19.

*Accepted for publication on September 09, 2025

†ebarbera@unime.it, Department of Mathematical, Computer, Physical and Earth Sciences, University of Messina, Italy, V.le F. Stagno D'Alcontres 31, I-98166 Messina, Italy

‡clfazio@unime.it, Department of Mathematical, Computer, Physical and Earth Sciences, University of Messina, Italy, V.le F. Stagno D'Alcontres 31, I-98166 Messina, Italy

1 Introduction

The description of physical phenomena in rarefied gases far from equilibrium is a relevant topic both from the theoretical and from the experimental point of view. It motivated many studies and experiments in order to catch the main features of the problem.

Stationary heat transfer in rarefied gases is the simplest non-equilibrium example, so it is always used to test and compare different approaches and methods. In some cases, the heat transfer problems were studied in a gas at rest, or sometimes in addition to Couette and Poiseuille flows to verify some particular properties of the models and to investigate the relation between the velocity and temperature fields.

Normally, the study of these phenomena is developed inside Classical Thermodynamics (CT) [20, 30], that is able to describe non-equilibrium phenomena under normal conditions. The fields of CT are the density, the velocity and the temperature. The field equations are based on the conservation laws of mass, momentum and energy that are closed by the Navier-Stokes and Fourier laws. It was shown that, for rarefied gases, the solutions of CT are not in complete agreement with the experiments or with the numerical integration of the Boltzmann equation [13, 34, 33]. Therefore, in these cases, a different theory must be taken into account.

It was shown that Rational Extended Thermodynamics [31, 36, 37] is able to predict a more reliable behavior than CT for rarefied gases or when strong deviations from the equilibrium state occur. Rational Extended Thermodynamics (RET) considers as fields not only the density, velocity and temperature but also the stress tensor and the heat flux and other non-equilibrium quantities. The field equations are based on balance equations, closed using universal physical principles, like the Entropy and the Galilean Principles. The field equations of RET form a symmetric hyperbolic system. Hyperbolicity guarantees finite speeds of propagation and symmetric hyperbolic systems have convenient and desirable mathematical properties, namely well-posedness of Cauchy problems, i.e. existence, uniqueness, and continuous dependence on the data.

In the particular case of rarefied gases, Rational Extended Thermodynamics moves very close to the Kinetic Theory. In fact, the fields are the moments of the distribution function and the balance equations are obtained directly from the Boltzmann equation [31]. The constitutive relations coincide with those obtained with the Grad's distribution function [25, 26].

Rational Extended Thermodynamics was tested in many physical examples and it turns out to be more suitable than Classical Thermodynamics for the description of rarefied gases; we recall, for example, light scattering [42], shock waves and shock structures [43], phonon theory [24]. Moreover, RET has been applied to relativistic phenomena [29], chemically reacting mixtures of gases [28] and radiation phenomena [38].

More recently, different studies on Rational Extended Thermodynamics have been carried out on heat transfer in gas mixtures, see [3] and in the references therein. The RET Theory was also generalized to dense and rarefied polyatomic gases, both in the classical [36, 37] and in the relativistic framework [35, 2, 1], and also different materials like metal electrons [4], quantum systems [39], graphene [40], blood flow [12], gas bubbles [15, 16, 17], nanofluids [11] and biological models [19, 27, 10], providing in all cases relevant results.

It has been shown [32] that Rational Extended Thermodynamics is different from Classical Thermodynamics for the heat transfer problem if the phenomenon takes place in a non-planar domain. Starting from the first results [32], different cases and different effects are studied, such as the study of non-inertial effects in a heat conduction problem in a rarefied gas [9] or in gas mixtures [3]. Then, stationary heat conduction in more complex 3D-domains is considered in the linearized case [6] or taking into account the non-linear terms [8]. Moreover, the heat transfer together with the axial [5] or helicoidal [7] flows between circular cylinders are investigated. In all studies, it was shown that the differences between Classical and Rational Extended Thermodynamics become more evident when the curvature of the domain is higher or when more complex effects are taken into account.

In this paper, starting from the previous results, the heat transfer problem in a rarefied gas together with Couette and Poiseuille flows in particular 3D-domains are investigated. The gas is in the gap between two elliptical cylinders or two circular non-coaxial cylinders. The simple stationary heat transfer problem in these 3D-domains was already investigated in [6]. Here the additional effect of the two flows is studied. The paper shows that in the linearized case, the velocity and temperature fields are uncoupled, so no differences between the heat transfer fields with or without flow can be highlighted. On the contrary, in the non-linear case, although the integration of the whole set of field equations is too complex, and a perturbation analysis, similar to the one carried out in [8], must be performed, interesting coupled effects arise. The solutions are shown and all effects of the different geometries and of the velocity field on the heat transfer problem are presented.

2 Field equations

In Kinetic Theory [18] the state of a gas is described by the phase density $f(\boldsymbol{x}, \boldsymbol{c}, t)$, such that

$$f(\boldsymbol{x}, \boldsymbol{c}, t)\mathrm{d}\boldsymbol{c} \tag{1}$$

represents the number of atoms at $\boldsymbol{x}$ and t with velocity between $\boldsymbol{c}$ and $\boldsymbol{c} + \mathrm{d}\boldsymbol{c}$.

In a monatomic gas, the phase density satisfies the well-known Boltzmann equation that, in an inertial frame, assumes the form

$$\frac{\partial f}{\partial t} + c_i \frac{\partial f}{\partial x_i} + f_i \frac{\partial f}{\partial c_i} = P, \tag{2}$$

where f_i is the specific external body force, and P is the collision operator that depends on the collisions between the atoms.

Grad's theory [25, 26] or Extended Thermodynamics of Moments [31] describes the state of the gas at a macroscopic level. They consider as fields variables the moments of the phase density, defined as

$$F_{i_1 i_2 \dots i_N} = m \int c_{i_1} c_{i_2} \dots c_{i_N} f \mathrm{d}\mathbf{c}, \tag{3}$$

where m is the atomic mass. In particular, for the rank "0" and "1" one has

$$\begin{aligned} F &= \rho, \\ F_i &= \rho v_i, \end{aligned} \tag{4}$$

being ρ the mass density of the gas and v_i its velocity. By use of v_i, it is possible to define the peculiar velocity $C_i = c_i - v_i$ and the internal moments:

$$\rho_{i_1 i_2 \dots i_N} = m \int C_{i_1} C_{i_2} \dots C_{i_N} f \mathrm{d}\mathbf{c}. \tag{5}$$

Some of these moments can be related to more common thermodynamic fields. Indeed, for the moment of rank "2", $\rho_{ij} = -t_{ij}$ holds, where t_{ij} is the stress tensor. Its trace is $\rho_{ll} = 3p = 3\frac{k_B}{m}\rho T$, where p is the pressure, k_B is the Boltzmann constant and T is the temperature. For the moment of third rank, one has $\rho_{ill} = 2q_i$, where q_i is the heat flux.

Multiplication of the Boltzmann equation (2) by $mc_{i_1} c_{i_2} \dots c_{i_N}$ and integration over all $\mathbf{c}$ give balance equations for the moments that, in the BGK [14] approximation, read

$$\frac{\partial F_{i_1 i_2 \dots i_N}}{\partial t} + \frac{\partial F_{i_1 i_2 \dots i_N k}}{\partial x_k} - N F_{(i_1 i_2 \dots i_{N-1}} f_{i_N)} = -\frac{F_{i_1 i_2 \dots i_N} - F^E_{i_1 i_2 \dots i_N}}{\tau}, \tag{6}$$

where τ is the constant relaxation time, the symbol "E" stands for the equilibrium value and round brackets in the indices indicate symmetrization.

Taking into account the definitions of peculiar velocity and of the moments (3, 5), it is possible to get the relations between $F_{i_1 i_2 \dots i_N}$ and $\rho_{i_1 i_2 \dots i_N}$, that can be written in the compact form:

$$F_{i_1 i_2 \dots i_N} = \sum_{k=1}^{N} \begin{pmatrix} N \\ k \end{pmatrix} \rho_{(i_1 i_2 \dots i_{N-k}} v_{i_{N-k+1}} \dots v_{i_N)}. \tag{7}$$

Substituting $F_{i_1 i_2 \dots i_N}$ from relations (7) into equations (6), it is possible to recover the balance equations for the internal moments that, in general, is an infinite hierarchy of balance equations for the $\rho_{i_1 i_2 \dots i_N}$.

It is common to consider only the first thirteen equations, since only the first thirteen moments have a clearly physical meaning. So the set of field equations becomes explicitly

$$\begin{aligned}
&\frac{\mathrm{d}\rho}{\mathrm{d}t} + \rho \frac{\partial v_k}{\partial x_k} = 0, \\
&\rho \frac{\mathrm{d}v_i}{\mathrm{d}t} + \frac{\partial \rho_{ik}}{\partial x_k} - \rho f_i = 0, \\
&\frac{\mathrm{d}\rho_{ij}}{\mathrm{d}t} + \rho_{ij} \frac{\partial v_k}{\partial x_k} + \frac{\partial \rho_{ijk}}{\partial x_k} + 2\rho_{(ki} \frac{\partial v_{j)}}{\partial x_k} = -\frac{\rho_{<ij>}}{\tau}, \\
&\frac{\mathrm{d}q_i}{\mathrm{d}t} + \frac{1}{2} \frac{\partial \rho_{ikll}}{\partial x_k} + q_i \frac{\partial v_k}{\partial x_k} + \frac{3}{2} \rho_{(il} \frac{\mathrm{d}v_{il)}}{\mathrm{d}t} + \frac{3}{2} \rho_{k(il} \frac{\partial v_{l)}}{\partial x_k} = -\frac{q_i}{\tau},
\end{aligned} \tag{8}$$

with $\mathrm{d}(\cdot)/\mathrm{d}t = \partial(\cdot)/\partial t + v_k \partial(\cdot)/\partial x_k$. The first two equations and the trace of the third represent respectively the conservation law of mass, momentum and energy. The traceless part of the third equation and the forth are balance laws for the traceless part of stress tensor and the heat flux.

System (8) consists of thirteen balance equations, for the thirteen fields: ρ, v_i, T, $\rho_{<ij>}$ and q_i. Unfortunately, it is not closed due to the presence of $\rho_{<ijk>}$ and ρ_{ikll}, which are not explicitly expressed in terms of the field variables. A possible way to close the system is using the Grad's distribution function [25, 26], which starts from an expansion of the phase density in terms of Hermite polynomials in C_i:

$$\begin{aligned}
f_G = f_E \Big[a - a_i \frac{m}{k_B T} C_i + a_{ij} \Big(\frac{m}{k_B T}\Big)^2 \Big(C_i C_j - \frac{k_B T}{m} \delta_{ij} \Big) + \\
- a_{ijk} \Big(\frac{m}{k_B T}\Big)^3 \Big(C_i C_j C_k - 3 \frac{k_B T}{m} \delta_{(ij} C_{k)} \Big) + \cdots \Big],
\end{aligned} \tag{9}$$

where f_E is the Maxwellian distribution function and the coefficients $\boldsymbol{a}$ must be determined.

Inserting (9) into the definitions (5) appropriate to the first thirteen moments, it is possible to get the coefficients $\boldsymbol{a}$'s explicitly in terms of the field variables. So the Grad's thirteen moments distribution function reads:

$$f_G = f_E\Big[1 + \frac{1}{2p}\frac{m}{k_B T}\rho_{<ij>}C_iC_j - \frac{1}{p}\frac{m}{k_B T}q_iC_i\Big(1 - \frac{1}{5}\frac{m}{k_B T}C^2\Big)\Big]. \tag{10}$$

By substitution of this distribution into the definition (5) appropriate to $\rho_{<ijk>}$ and ρ_{ikll} it follows

$$\begin{aligned} \rho_{<ijk>} &= 0, \\ \rho_{ikll} &= 5p\frac{k_B}{m}T\delta_{ik} + 7\frac{k_B}{m}T\rho_{<ik>}. \end{aligned} \tag{11}$$

These are the required constitutive relations. Then, substituting (11) into the balance equations (8), it is possible to obtain the closed system of field equations in terms of the fields. It can be integrated under particular conditions and every solution is called a Thermodynamic Process.

3 Geometrical description of the problem

In this paper, we consider the stationary heat transfer in a classical ideal monoatomic gas together with two different kind of flows inside two different 3D-domains. Indeed, as explained in the introduction, we study the Couette and Poiseuille flows between two confocal elliptical cylinders and two non-coaxial cylinders. In order to describe these flows, we introduce two different and appropriate sets of orthogonal coordinates indicated with (z^1, z^2, z^3).

3.1 Confocal elliptical cylinders

Elliptical cylindrical coordinates [44] are related to the Cartesian ones by

$$\begin{aligned} x_1 &= c\cosh z^1 \cos z^2, \\ x_2 &= c\sinh z^1 \sin z^2, \\ x_3 &= z^3, \end{aligned} \tag{12}$$

where the length $2c$ represents the distance between the common foci and

$$z_i^1 \le z^1 \le z_e^1 \qquad 0 \le z^2 < 2\pi \qquad -\infty < z^3 < \infty. \tag{13}$$

The coordinate surfaces are

$$
\begin{aligned}
\frac{x_1^2}{\cosh^2 z^1} + \frac{x_2^2}{\sinh^2 z^1} &= c^2, \\
\frac{x_1^2}{\cos^2 z^2} - \frac{x_2^2}{\sin^2 z^2} &= c^2, \\
x_3 &= z^3.
\end{aligned} \tag{14}
$$

Their intersection with the plane $x_3 = 0$ is illustrated in Fig.1(left). For this set of coordinates, the metric tensor is diagonal and its non-vanishing components are

$$
g^{11} = g^{22} = g = \frac{2}{c^2} \frac{1}{\cosh(2z^1) - \cos(2z^2)}, \quad g^{33} = 1. \tag{15}
$$

Moreover, the non vanishing Christoffel symbols become

$$
\begin{aligned}
\Gamma^1_{11} = -\Gamma^1_{22} = \Gamma^2_{12} = \Gamma^2_{21} &= \frac{\sinh(2z^1)}{\cosh(2z^1) - \cos(2z^2)}, \\
\Gamma^2_{22} = -\Gamma^2_{11} = \Gamma^1_{12} = \Gamma^1_{21} &= \frac{\sin(2z^2)}{\cosh(2z^1) - \cos(2z^2)}.
\end{aligned} \tag{16}
$$

3.2 Non-coaxial circular cylinders

Another set of orthogonal coordinates, used here in order to describe this heat conduction problem between two non-coaxial circular cylinders, are the bi-cylindrical coordinates [44]. These are related to the Cartesian one by:

$$
\begin{aligned}
x_1 &= c \frac{\sinh z^1}{\cosh z^1 - \cos z^2}, \\
x_2 &= c \frac{\sin z^2}{\cosh z^1 - \cos z^2}, \\
x_3 &= z^3,
\end{aligned} \tag{17}
$$

with

$$
z_e^1 \le z^1 \le z_i^1, \qquad 0 \le z^2 \le 2\pi, \qquad -\infty \le z^3 \le \infty. \tag{18}
$$

The coefficient c is related to the radii of the internal circles, a, and external b, respectively

$$
a = \frac{c}{\sinh z_i^1}, \qquad b = \frac{c}{\sinh z_e^1}. \tag{19}
$$

Moreover, if d is the distance between the centers of the circles, it follows:

$$
c^2 = \frac{1}{4d^2} \left[(d^2 - a^2 - b^2)^2 - 4a^2 b^2 \right]. \tag{20}
$$

The coordinate surfaces are:

$$\begin{aligned} &(x_1 + c\coth z^1)^2 + x_2^2 = c^2(\coth^2 z^1 - 1), \\ &x_1^2 + (x_2 - c\cot z^2)^2 = c^2(\cot^2 z^2 + 1), \\ &x_3 = z^3. \end{aligned} \tag{21}$$

Their intersection with the plane $x_3 = 0$ is shown in Fig.1(right). Also in this case the metric tensor is diagonal:

$$g^{11} = g^{22} = g = \frac{1}{c^2}(\cos z^2 - \cosh z^1)^2, \quad g^{33} = 1; \tag{22}$$

while, the non-vanishing Christoffel symbols assume the form

$$\begin{aligned} \Gamma^1_{11} = -\Gamma^1_{22} = \Gamma^2_{12} = \Gamma^2_{21} = \tfrac{\sinh z^1}{\cos z^2 - \cosh z^1}, \\ \Gamma^2_{22} = -\Gamma^2_{11} = \Gamma^1_{12} = \Gamma^1_{21} = \tfrac{\sin z^2}{\cos z^2 - \cosh z^1}. \end{aligned} \tag{23}$$

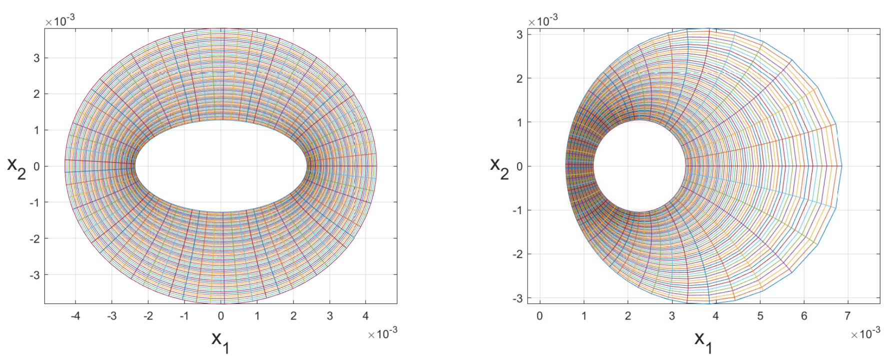

Figure 1: An illustration of both the coordinates: confocal elliptical cylinders on the left and non-coaxial circular ones on the right.

4 Dimensionless field equations

In both geometries, a stationary phenomena is considered. Furthermore it is assumed that the flow occurs in z^3-direction, coincident with the cylinders axis, so only the third component of the velocity doesn't vanish and all fields depend only on z^1 and z^2-coordinates. Then, in terms of the physical components of the tensor [36, 41], we introduce the dimensionless variables

$$\tilde{p} = \frac{p}{p_e}, \qquad \tilde{T} = \frac{T}{T_e}, \qquad \tilde{\rho}^{<ij>} = \frac{\rho^{<ij>}}{p_e}, \qquad \tilde{g} = c^2 g,$$
$$\tilde{q}^i = \frac{q^i}{p_e\sqrt{\frac{k_B}{m}T_e}}, \qquad \tilde{v}^i = \frac{v^i}{\sqrt{\frac{k_B}{m}T_e}}, \qquad Kn = \frac{\tau}{c}\sqrt{\frac{k_B}{m}T_e}, \tag{24}$$

where p_e and T_e are the pressure and the temperature at the external boundary, respectively. Kn is the parameter of the problem. It is proportional to the Knudsen number, that is a dimensionless number defined as the ratio between the molecular mean free path length and a representative physical length scale. Kn is a good measure for the degree of gas rarefaction.
In terms of the dimensionless field variables, under the previous assumptions, the field equations become

$$\begin{aligned}
&\tfrac{\partial\tilde{p}}{\partial z^1} + \tfrac{\partial\tilde{\rho}^{<11>}}{\partial z^1} + \tfrac{\partial\tilde{\rho}^{<12>}}{\partial z^2} + \Gamma^1_{11}\tilde{\rho}^{<11>} - \Gamma^1_{11}\tilde{\rho}^{<22>} + 2\Gamma^2_{22}\tilde{\rho}^{<12>} = 0,\\
&\tfrac{\partial\tilde{p}}{\partial z^2} + \tfrac{\partial\tilde{\rho}^{<12>}}{\partial z^1} + \tfrac{\partial\tilde{\rho}^{<22>}}{\partial z^2} + \Gamma^2_{22}\tilde{\rho}^{<22>} - \Gamma^2_{22}\tilde{\rho}^{<11>} + 2\Gamma^1_{11}\tilde{\rho}^{<12>} = 0,\\
&\tfrac{\partial\tilde{\rho}^{<13>}}{\partial z^1} + \tfrac{\partial\tilde{\rho}^{<23>}}{\partial z^2} + \Gamma^1_{11}\tilde{\rho}^{<13>} + \Gamma^2_{22}\tilde{\rho}^{<23>} = -\tilde{\varphi},\\
&\tfrac{6}{5}\tfrac{\partial\tilde{q}^1}{\partial z^1} + \tfrac{2}{5}\tfrac{\partial\tilde{q}^2}{\partial z^2} + \tfrac{2}{5}\Gamma^1_{11}\tilde{q}^1 + \tfrac{6}{5}\Gamma^2_{22}\tilde{q}^2 = -\tfrac{\tilde{\rho}^{<11>}}{Kn\sqrt{\tilde{g}}},\\
&\tfrac{2}{5}\tfrac{\partial\tilde{q}^1}{\partial z^1} + \tfrac{6}{5}\tfrac{\partial\tilde{q}^2}{\partial z^2} + \tfrac{6}{5}\Gamma^1_{11}\tilde{q}^1 + \tfrac{2}{5}\Gamma^2_{22}\tilde{q}^2 = -\tfrac{\tilde{\rho}^{<22>}}{Kn\sqrt{\tilde{g}}},\\
&\tfrac{\partial\tilde{q}^1}{\partial z^1} + \tfrac{\partial\tilde{q}^2}{\partial z^2} + \Gamma^1_{11}\tilde{q}^1 + \Gamma^2_{22}\tilde{q}^2 \underline{+\rho_{<13>}\tfrac{\partial\tilde{v}^3}{\partial z^1} + \rho_{<23>}\tfrac{\partial\tilde{v}^3}{\partial z^2}} = 0,\\
&\tfrac{2}{5}\tfrac{\partial\tilde{q}^2}{\partial z^1} + \tfrac{2}{5}\tfrac{\partial\tilde{q}^1}{\partial z^2} - \tfrac{2}{5}\Gamma^1_{11}\tilde{q}^2 - \tfrac{2}{5}\Gamma^2_{22}\tilde{q}^1 = -\tfrac{\tilde{\rho}^{<12>}}{Kn\sqrt{\tilde{g}}},\\
&\tfrac{2}{5}\tfrac{\partial\tilde{q}^3}{\partial z^1} + \tilde{p}\tfrac{\partial\tilde{v}^3}{\partial z^1} \underline{+\tilde{\rho}^{<11>}\tfrac{\partial\tilde{v}^3}{\partial z^1} + \tilde{\rho}^{<12>}\tfrac{\partial\tilde{v}^3}{\partial z^2}} = -\tfrac{\tilde{\rho}^{<13>}}{Kn\sqrt{\tilde{g}}},\\
&\tfrac{2}{5}\tfrac{\partial\tilde{q}^3}{\partial z^2} + \tilde{p}\tfrac{\partial\tilde{v}^3}{\partial z^2} \underline{+\tilde{\rho}^{<22>}\tfrac{\partial\tilde{v}^3}{\partial z^2} + \tilde{\rho}^{<12>}\tfrac{\partial v^3}{\partial z^1}} = -\tfrac{\tilde{\rho}^{<23>}}{Kn\sqrt{\tilde{g}}},\\
&7\underline{\tilde{\rho}^{<11>}\tfrac{\partial\tilde{T}}{\partial z^1} + 7\tilde{\rho}^{<12>}\tfrac{\partial\tilde{T}}{\partial z^2}} - 2\underline{\tilde{T}}\tfrac{\partial\tilde{p}}{\partial z^1} + 5\underline{\tilde{p}}\tfrac{\partial\tilde{T}}{\partial z^1} + \underline{\tfrac{4}{5}\tilde{q}^3\tfrac{\partial\tilde{v}^3}{\partial z^1}} = -2\tfrac{\tilde{q}^1}{Kn\sqrt{\tilde{g}}},\\
&7\underline{\tilde{\rho}^{<12>}\tfrac{\partial\tilde{T}}{\partial z^1} + 7\tilde{\rho}^{<22>}\tfrac{\partial\tilde{T}}{\partial z^2}} - 2\underline{\tilde{T}}\tfrac{\partial\tilde{p}}{\partial z^2} + 5\underline{\tilde{p}}\tfrac{\partial\tilde{T}}{\partial z^2} + \underline{\tfrac{4}{5}\tilde{q}^3\tfrac{\partial\tilde{v}^3}{\partial z^2}} = -2\tfrac{\tilde{q}^2}{Kn\sqrt{\tilde{g}}},\\
&7\underline{\tilde{\rho}^{<13>}\tfrac{\partial\tilde{T}}{\partial z^1} + 7\tilde{\rho}^{<23>}\tfrac{\partial\tilde{T}}{\partial z^2} + \tfrac{14}{5}\tilde{q}^1\tfrac{\partial\tilde{v}^3}{\partial z^1} + \tfrac{14}{5}\tilde{q}^2\tfrac{\partial\tilde{v}^3}{\partial z^2}} = -2\tfrac{\tilde{q}^3}{Kn\sqrt{\tilde{g}}},
\end{aligned} \tag{25}$$

In the following, we will present some solutions of equations (25) assuming as dimensionless boundary conditions the pressure $\tilde{p}_e = 1$, the internal and external boundary temperatures $\tilde{T}_i = 1.15$ and $\tilde{T}_e = 1$.

In addiction, for the Couette problem, we will consider different values for the velocity at the internal boundary is $\tilde{v}_i$, while at external cylinder we will have $\tilde{v}_e = 0$. For the Poiseuille problem, we will consider both $\tilde{v}_i = \tilde{v}_e = 0$ and the flow will be generated by external force $\tilde{\varphi}$.

5 Linearized field equations

A possible way to obtain a particular solution of these problems is to linearize the system of field equations (25) around an equilibrium state characterized by $\tilde{p}_0 = 1$, $\tilde{T}_0 = 1$, $\tilde{\rho}_0^{<ij>} = 0$ and $\tilde{q}_0^i = 0$. In this case, the system of field equations coincides with the set (25) where the underlined terms are neglected.

Manipulating this system, it is possible to obtain the analytic solution: the pressure $\tilde{p}$ is constant and equal to the boundary value $\tilde{p}_e = 1$;

$$\tilde{p} = 1, \tag{26}$$

the temperature and the velocity fields must satisfy the following Laplace or Poisson equations

$$\begin{aligned} \Delta\tilde{T} &= \tfrac{\partial^2\tilde{T}}{\partial(z^1)^2} + \tfrac{\partial^2\tilde{T}}{\partial(z^2)^2} = 0, \\ \Delta\tilde{v}^3 &= \tfrac{\partial^2\tilde{v}^3}{\partial(z^1)^2} + \tfrac{\partial^2\tilde{v}^3}{\partial(z^2)^2} = -\tilde{\varphi}, \end{aligned} \tag{27}$$

where $\Delta(\cdot)$ is the Laplace operator in the (z^1, z^2)-coordinates. The last equation is the Laplace equation for the Couette flow ($\tilde{\varphi} = 0$) or a Poisson equation for Poseuille flow. These equations must be integrated with the appropriate boundary conditions. Once the solutions for $\tilde{T}$ and $\tilde{v}^3$ is known, they can be inserted in the remaining linearized equations $(25)_{8-12}$, that can be written in the more compact form as

$$\begin{aligned} \tilde{q}^1 &= -\tfrac{5}{2} Kn\sqrt{\tilde{g}}\tfrac{\partial\tilde{T}}{\partial z^1}, \\ \tilde{q}^2 &= -\tfrac{5}{2} Kn\sqrt{\tilde{g}}\tfrac{\partial\tilde{T}}{\partial z^2}, \\ \tilde{q}^3 &= 0, \\ \rho^{<13>} &= -Kn\sqrt{\tilde{g}}\tfrac{\partial\tilde{v}^3}{\partial z^1}, \\ \rho^{<23>} &= -Kn\sqrt{\tilde{g}}\tfrac{\partial\tilde{v}^3}{\partial z^2}. \end{aligned} \tag{28}$$

These equations coincide with the classical Navier-Stokes and Fourier assumptions, so no difference can be detected for these fields using the linear

RET equations. On the contrary, inserting the temperature field in the last linearized equations $(25)_{4,5,7}$, it follows

$$\begin{aligned}
\rho^{<11>} &= -\rho^{<22>} = -2Kn^2\tilde{g}\Big(\Gamma^1_{11}\tfrac{\partial\tilde{T}}{\partial z^1} - \Gamma^2_{22}\tfrac{\partial\tilde{T}}{\partial z^2} - \tfrac{\partial^2\tilde{T}}{\partial(z^1)^2}\Big),\\
\rho^{<12>} &= -2Kn^2\tilde{g}\Big(\Gamma^2_{22}\tfrac{\partial\tilde{T}}{\partial z^1} + \Gamma^1_{11}\tfrac{\partial\tilde{T}}{\partial z^2} - \tfrac{\partial^2\tilde{T}}{\partial z^1\partial z^2}\Big),
\end{aligned}\tag{29}$$

and for these quantities we get the differences from the classical solutions. Indeed, Navier-Stokes and Fourier assumptions neglect the existence of non-vanishing $\rho^{<11>}$, $\rho^{<22>}$ and $\rho^{<12>}$ components. Here, instead, we get small but non-vanishing traceless parts of the stress tensor that depend on the temperature field.

Due to the geometry of the domains and the boundary conditions on the fields, it is possible to assume the temperature and velocity as dependent only on the z^1-coordinate. In this way, equations $(27)_{2,3}$ can be easily integrated in order to get

$$\begin{aligned}
\tilde{T} &= T_i + \frac{\tilde{T}_e - \tilde{T}_i}{z^1_e - z^1_i}(z^1 - z^1_i),\\
\tilde{v}^3 &= -\frac{\tilde{\varphi}}{2}(z^1)^2 + \frac{\tilde{\varphi}(z^1_e)^2 - \tilde{\varphi}(z^1_i)^2 + 2\tilde{v}_e - 2\tilde{v}_i}{2(z^e_1 - z^i_1)}z^1 +\\
&\quad + \frac{-\tilde{\varphi}(z^1_e)^2 z^1_i + \tilde{\varphi}z^1_e(z^1_i)^2 - 2\tilde{v}_e z^1_i + 2\tilde{v}_i z^1_e}{2(z^1_e - z^1_i)},
\end{aligned}\tag{30}$$

and, from (28) and (29), it follows

$$\begin{aligned}
\tilde{q}^1 &= -\frac{5}{2}Kn\sqrt{\tilde{g}}\frac{\tilde{T}_e - \tilde{T}_i}{z^1_e - z^1_i},\\
\tilde{\rho}^{<11>} &= -\tilde{\rho}^{<22>} = -2Kn^2\tilde{g}\Gamma^1_{11}\frac{\tilde{T}_e - \tilde{T}_i}{z^1_e - z^1_i},\\
\tilde{\rho}^{<12>} &= -2Kn^2\tilde{g}\Gamma^2_{22}\frac{\tilde{T}_e - \tilde{T}_i}{z^1_e - z^1_i},\\
\tilde{\rho}^{<13>} &= -Kn\sqrt{\tilde{g}}\Big[-\tilde{\varphi}z^1 + \frac{\tilde{\varphi}(z^1_e)^2 - \tilde{\varphi}(z^1_i)^2 + 2\tilde{v}_e - 2\tilde{v}_i}{2(z^1_e - z^1_i)}\Big],\\
\tilde{q}^2 &= \tilde{\rho}^{<23>} = \tilde{q}^3 = 0.
\end{aligned}\tag{31}$$

In these solutions, the temperature and the velocity fields depend only on z^1, while, for the other fields, the dependence on z^2 and on the geometry occurs through the variables $\tilde{g}$, Γ^1_{11} and Γ^2_{22}.

From (30), it is clear that in both geometries the temperature is a linear function of z^1, while $\tilde{v}^3$ is a quadratic function of z^1. This means that in the first geometry $\tilde{T}$ increase linearly in the hyperboles $(14)_2$, and it remains constant in the ellipses $(14)_1$. Instead, in the other geometry $\tilde{T}$ increase linearly in the circumferences $(21)_2$ while it is constant in $(21)_1$.

In Figs.2,3 (upper figures) we illustrate the temperature field $(30)_1$ together with the corresponding heat flux $\tilde{q}^1$ in $(31)_1$, appropriate to the two different geometries for the Poiseuille flow.

The temperature and the heat flux coincide with the Fourier solutions and they depend only on the geometry of the problem and not on the velocity field.

In Figs.2,3 (middle) we show the velocity field $(30)_2$ and the corresponding stress tensor component $\tilde{\rho}^{<13>}$ in $(31)_4$, that coincide with the prediction of Navier-Stokes flow. Finally, in Figs.2,3 (bottom) we show the additional fields $\tilde{\rho}^{<11>} = -\tilde{\rho}^{<22>}$ and $\tilde{\rho}^{<12>}$ for the different geometries. The existence of these new non-vanishing components of the stress tensor was already obtained in [6]. They are additive stresses that depend only on temperature field and not on the velocity field. Since, due to the linearization, the temperature and the velocity fields are uncoupled and the solution for $\tilde{T}$ and $\tilde{q}^1$ for the Couette flow coincide with the solution for Poiseuille flow illustrated in Figs.2,3 (upper). Instead, in Figs.4,5, we show the velocity field $\tilde{v}^3$ in $(30)_2$ and the corresponding stress tensor component $\tilde{\rho}^{<13>}$ in $(31)_4$ for the two different geometries. Finally, also for the Couette flow, there are present the additional stress tensor components $\tilde{\rho}^{<11>} = -\tilde{\rho}^{<22>}$ and $\tilde{\rho}^{<12>}$ that don't depend on the velocity field so they coincide with the solution for the Poiseuille flow illustrated in Figs.2,3 (bottom).

These fields are the only differences from the Classical Thermodynamic solutions that can be obtained for the geometries here in consideration and with the chosen boundary conditions. It is remarkable that they can be already observed in the linearized case. In order to recover more precise effects, we will present in the next section some non-linear effects.

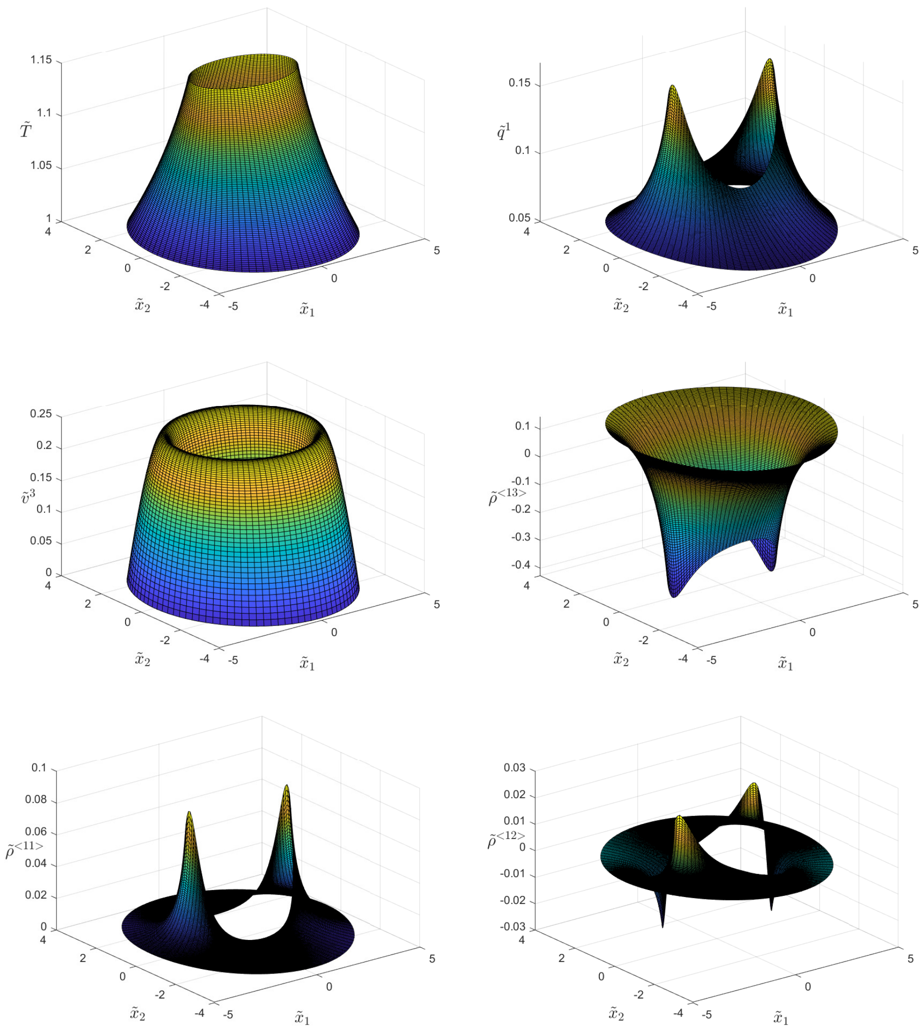

Figure 2: Solutions of the linearized field equations (27)-(29) for Poiseuille flow with $\tilde{\varphi} = 3$ in elliptical cylindrical coordinates.

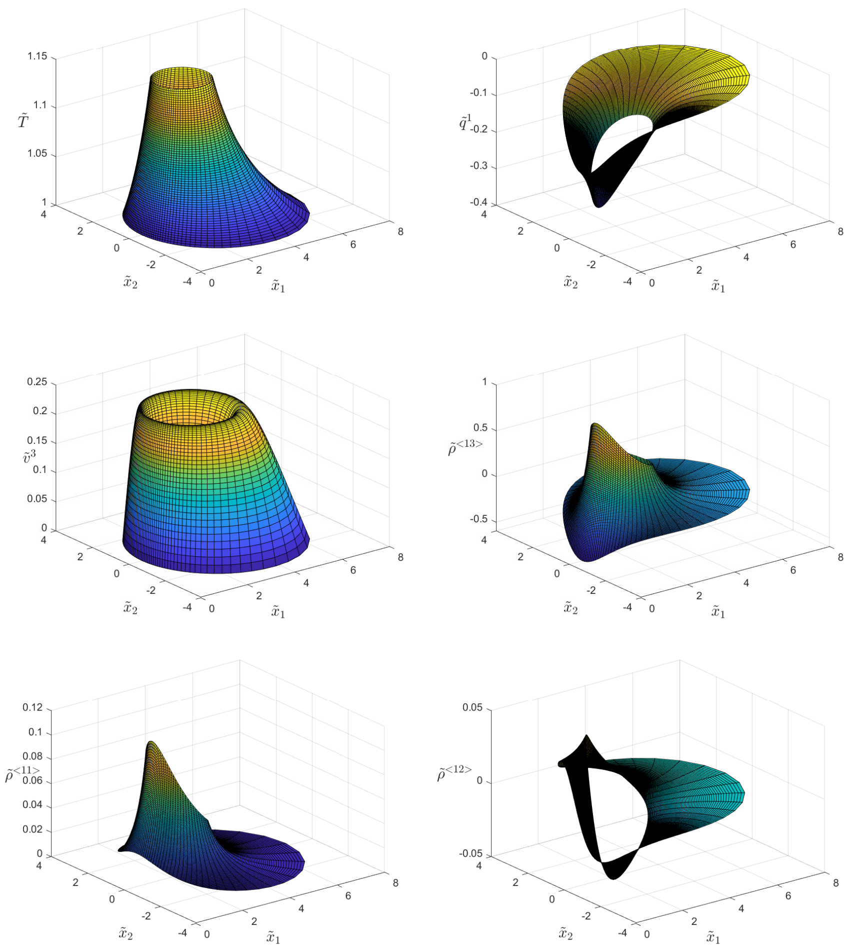

Figure 3: Solutions of the linearized field equations (27)-(29) for Poiseuille flow with $\tilde{\varphi} = 3$ in bi-cylindrical coordinates.

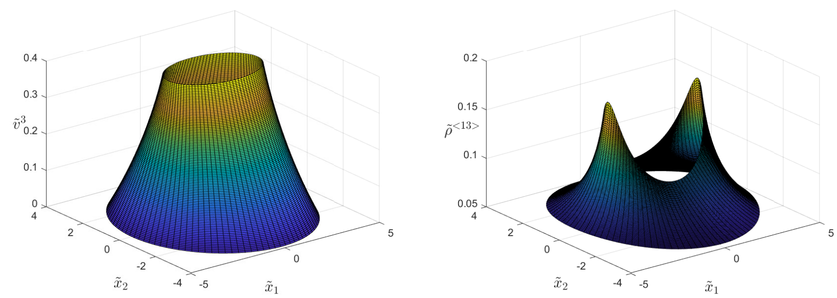

Figure 4: Solutions of the linearized field equations (27)-(29) for Couette flow with $\tilde{v}_i = 0.4$ in elliptical cylindrical coordinates. The temperature, the heat flux, $\tilde{\rho}^{<11>}$, $\tilde{\rho}^{<12>}$ coincide with the correspondent solutions in Fig. 2.

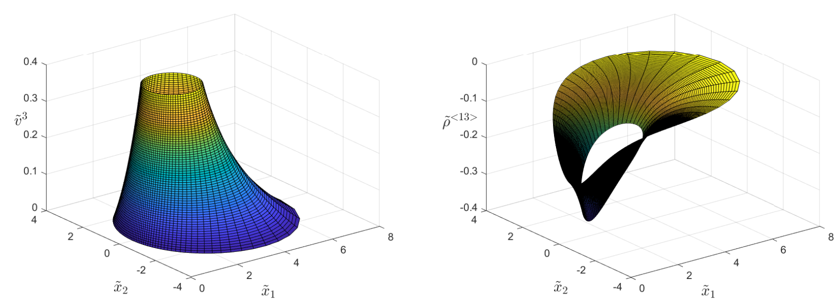

Figure 5: Solutions of the linearized field equations (27)-(29) Couette flow with $\tilde{v}_i = 0.4$ in bi-cylindrical coordinates. The temperature, the heat flux, $\tilde{\rho}^{<11>}$, $\tilde{\rho}^{<12>}$ coincide with the correspondent solutions in Fig. 3.

6 Reductive perturbation method

In this section, we consider a reductive perturbation method in order to get a more detailed description of the problem that takes into account some non-linear effects, too. In this paper we want to describe the behavior of a rarefied gas, therefore Kn is small ($Kn \ll 1$). In this way, it is possible to express the dimensionless fields as the sum of power series in Kn:

$$\begin{aligned} &\tilde{p} = \sum_{s\geq 0} Kn^s \tilde{p}^{(s)}, \qquad \tilde{T} = \sum_{s\geq 0} Kn^s \tilde{T}^{(s)}, \qquad \tilde{v}^i = \sum_{s\geq 0} Kn^s \tilde{v}^{i(s)}, \\ &\tilde{\rho}^{<ij>} = \sum_{s\geq 0} Kn^s \tilde{\rho}^{<ij>(s)}, \qquad \tilde{q}^i = \sum_{s\geq 0} Kn^s \tilde{q}^{i(s)}. \end{aligned} \tag{32}$$

We insert these representations in the field equations (25) equating all terms of the same order, to get the different orders fields in both Poiseuille and Couette flow.

For the 0^{th} order it follows:

$$\frac{\partial \tilde{p}^{(0)}}{\partial z^1} = 0, \qquad \frac{\partial \tilde{p}^{(0)}}{\partial z^2} = 0, \tag{33}$$

and, integrating these equations, with the boundary condition $\tilde{p}^{(0)}(z_e^1, z^2) = 1$, we get the solution

$$\tilde{p}^{(0)}(z^1, z^2) = 1. \tag{34}$$

While, for the velocity and temperature fields $\tilde{v}^{3(0)}$ and $\tilde{T}^{(0)}$, we obtain from system (25), the following Poisson equations:

$$\begin{aligned} &\frac{\partial^2 \tilde{v}^{3(0)}}{\partial (z^1)^2} + \frac{\partial^2 \tilde{v}^{3(0)}}{\partial (z^2)^2} = -\tilde{\varphi}, \\ &\frac{\partial^2 \tilde{T}^{(0)}}{\partial (z^1)^2} + \frac{\partial^2 \tilde{T}^{(0)}}{\partial (z^2)^2} + \frac{2}{5}\left(\frac{\partial \tilde{v}^{3(0)}}{\partial z^1}\right)^2 + \frac{2}{5}\left(\frac{\partial \tilde{v}^{3(0)}}{\partial z^2}\right)^2 = 0 \end{aligned} \tag{35}$$

that can be easily analytically integrated with appropriate boundary conditions. For Poiseuille flow, we assume

$$\begin{aligned} &\tilde{T}^{(0)}(z_i^1, z^2) = \tilde{T}_i, \qquad \tilde{T}^{(0)}(z_e^1, z^2) = \tilde{T}_e, \\ &\tilde{v}^{3(0)}(z_i^1, z^2) = 0, \qquad \tilde{v}^{3(0)}(z_e^1, z^2) = 0, \end{aligned} \tag{36}$$

in order to get, by integration of (35), the following solutions

$$\begin{aligned} &\tilde{v}^{3(0)}(z^1) = -A(z^1)^2 - Bz^1 + C, \\ &\tilde{T}^{(0)}(z^1) = -\frac{1}{15}\frac{(2Az^1 + B)^4}{8A^2} + Dz^1 + E, \end{aligned} \tag{37}$$

where the constants A-E are evaluated setting the boundary conditions (36):

$$\begin{aligned} &A = \frac{\tilde{\varphi}}{2}, \quad B = -\frac{\tilde{\varphi}}{2}\left(z_e^1 + z_i^1\right), \quad C = -\frac{\tilde{\varphi}}{2} z_e^1 z_i^1, \\ &D = \frac{\tilde{T}_e - \tilde{T}_i}{z_e^1 - z_i^1} + \frac{1}{60A^2}\left[\frac{(2Az_e^1 + B)^4 - (2Az_i^1 + B)^4}{2(z_e^1 - z_i^1)}\right], \\ &E = \tilde{T}_i + \frac{1}{60}\frac{(2Az_i^1 + B)^4}{2A^2} - Dz_i^1. \end{aligned} \tag{38}$$

As it can be noticed, the temperature is not anymore a linear function but its behavior is affected by the velocity field. This non-linear effect is the first difference from the linearized solution (30).

In Fig.6 the velocity $\tilde{v}^{3(0)}$ and the temperature $\tilde{T}^{(0)}$ are illustrated for different labeled values of $\tilde{\varphi}$. The figures refer to both geometries. Velocity coincides with the linearized solution $(30)_2$, the temperature solution depends on the velocity field.

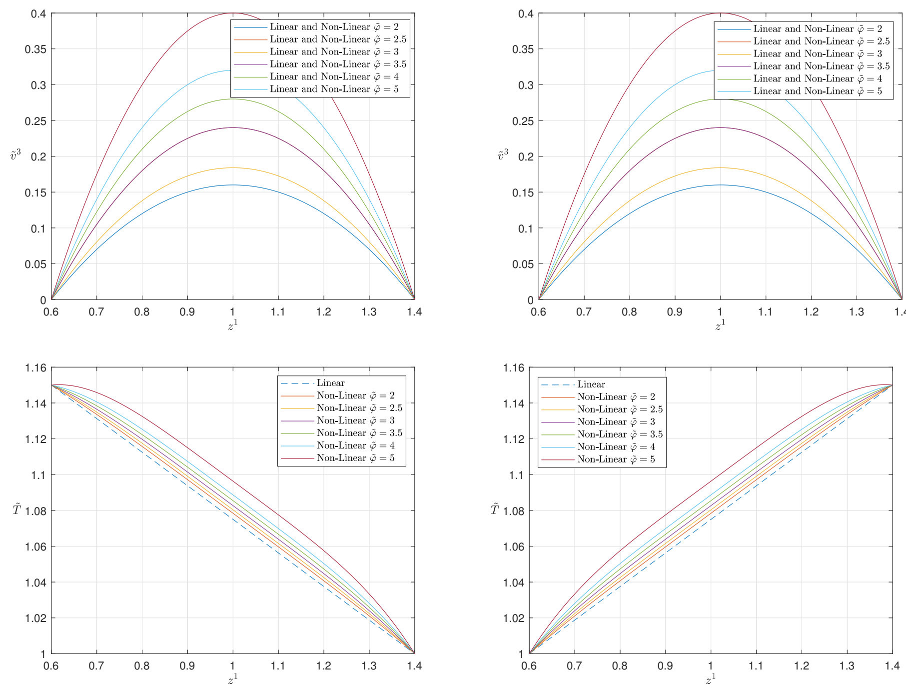

Figure 6: Poiseuille flow. Velocity and temperature in the linearized case and zeroth-order as the force $\tilde{\varphi}$ varies between 2 and 5. Left: confocal elliptical cylinders. Right: non-coaxial circular cylinders.

For the Couette flow, we set $\tilde{\varphi} = 0$ in (35) and we consider the following boundary conditions:

$$\begin{aligned} &\tilde{T}^{(0)}(z_i^1, z^2) = \tilde{T}_i, \qquad && \tilde{T}^{(0)}(z_e^1, z^2) = \tilde{T}_e, \\ &\tilde{v}^{3(0)}(z_i^1, z^2) = \tilde{v}_i, \qquad && \tilde{v}^{3(0)}(z_e^1, z^2) = \tilde{v}_e = 0. \end{aligned} \tag{39}$$

Hence the non-vanishing 0^{th} order variables appropriate to this flow, can be written as

$$\tilde{v}^{3(0)}(z^1) = Lz^1 + G,$$
$$\tilde{T}^{(0)}(z^1) = -\frac{L^2}{5}(z^1)^2 + \left[H + \frac{L^2}{5}(z_e^1 + z_i^1)\right]z^1 + \frac{\tilde{T}_i z_e^1 - \tilde{T}_e z_i^1}{z_e^1 - z_i^1} - \frac{L^2}{5} z_e^1 z_i^1, \tag{40}$$

where the integrating constants are

$$L = \frac{\tilde{v}_e - \tilde{v}_i}{z_e^1 - z_i^1}, \quad G = \frac{z_e^1 \tilde{v}_i - z_i^1 \tilde{v}_e}{z_e^1 - z_i^1}, \quad H = \frac{\tilde{T}_e - \tilde{T}_i}{z_e^1 - z_i^1}. \tag{41}$$

Fig.7 illustrates the velocity and the temperature appropriate to Couette flow at zeroth order. As before, the velocity still coincides with the linearized case, while, the temperature shows non-linear effects, due the presence of the velocity field.

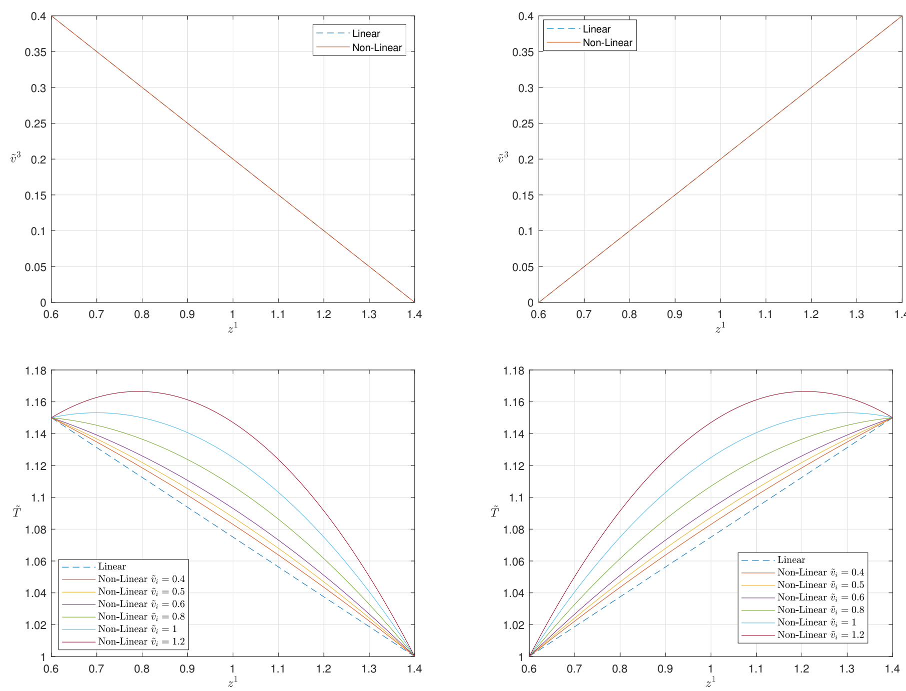

Figure 7: Couette flow. Velocity and temperature in the linearized case and the 0^{th} order as $\tilde{v}_i$ varies between 0.4 and 1.2. Left: confocal elliptical cylinders. Right: non-coaxial circular cylinders.

The first order non-vanishing terms can be easily obtained from

$$\begin{aligned}\tilde{q}^{1(1)}(z^1, z^2) &= -\frac{5}{2} Kn \sqrt{\tilde{g}} \frac{\partial \tilde{T}^{(0)}}{\partial z^1}, \\ \tilde{\rho}^{<13>(1)}(z^1, z^2) &= -Kn \sqrt{\tilde{g}} \frac{\partial \tilde{v}^{3(0)}}{\partial z^1},\end{aligned} \tag{42}$$

that result from the first order terms in the field equations (25). These equations coincide with the classical Navier-Stokes and Fourier equations. So no differences between the Grad's and the classical solutions can be appreciate in the first order. The solutions of equations (42) are illustrated in Figs.8-9 for the different symmetries and the different flows. These figures show that the stress tensor component $\tilde{\rho}^{<13>}$ coincides in all cases with the corresponding linearized solution, since the velocity is the same of the linearized case. Instead, heat flux component $\tilde{q}^{1(1)}$ differs from the linearized solution, since the temperature field doesn't coincide exactly with the linearized one, but it depends on the velocity field.

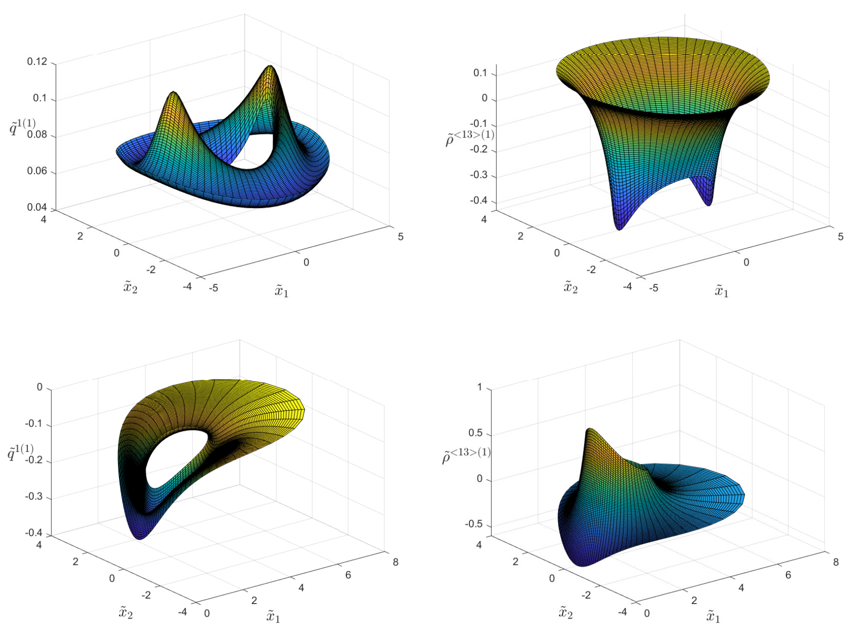

Figure 8: (above) Elliptical cylindrical coordinates and (below) bi-cylindrical coordinates in Poiseuille Problem with $\tilde{\varphi} = 3$.

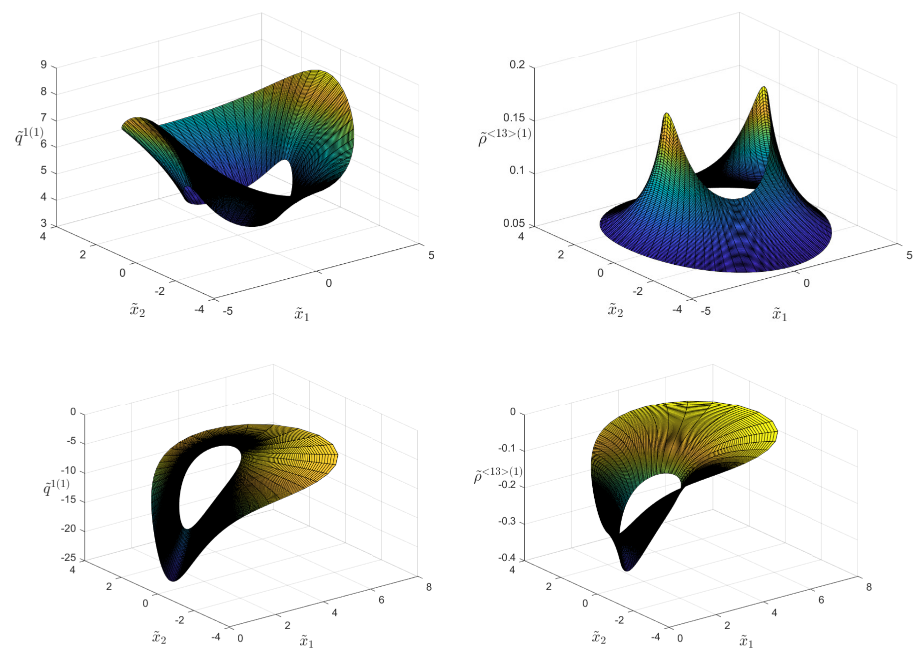

Figure 9: (above) Elliptical cylindrical coordinates and (below) bi-cylindrical coordinates in Couette Problem.

Finally, for the second order terms, we have two differential equations for the pressure $\tilde{p}^{(2)}$:

$$\begin{aligned}\frac{\partial \tilde{p}^{(2)}}{\partial z^1} &= 3Kn^2\tilde{g}\left[2\Gamma^1_{11}\frac{\partial^2\tilde{T}^{(0)}}{\partial (z^1)^2} - \frac{\partial^3\tilde{T}^{(0)}}{\partial (z^1)^3}\right],\\ \frac{\partial \tilde{p}^{(2)}}{\partial z^2} &= 6Kn^2\Gamma^2_{22}\tilde{g}\frac{\partial^2\tilde{T}^{(0)}}{\partial (z^1)^2}.\end{aligned} \tag{43}$$

Their solution reads

$$\tilde{p}^{(2)}(z^1, z^2) = Kn^2\left[P + \frac{6}{5}\tilde{g}\Big(\frac{\partial \tilde{v}^3}{\partial z^1}\Big)^2\right], \tag{44}$$

where P is the integration constant that must be evaluated according to the condition $\tilde{p}^{(2)}(z^1_e, z^2) = 0$.

From the remaining equations in (25) we get

$$\begin{aligned}&\tilde{q}^{1(2)} = \tilde{q}^{2(2)} = 0,\\ &\tilde{\rho}^{<13>(2)} = \tilde{\rho}^{<23>(2)} = 0.\end{aligned} \tag{45}$$

Therefore, in the second order there are no differences in the two component of the heat flux $\tilde{q}^1$ and $\tilde{q}^2$ and of the stress tensor $\tilde{\rho}^{<13>}$ and $\tilde{\rho}^{<23>}$ from the classical Fourier and Navier-Stokes. Instead, already at second order, we have new non-vanishing components of the heat flux and stress tensor:

$$\begin{aligned}
&\tilde{q}^{3(2)}(z^1,z^2) = 7Kn^2\tilde{g}\frac{\partial \tilde{v}^{3(0)}}{\partial z^1}\frac{\partial \tilde{T}^{(0)}}{\partial z^1},\\
&\tilde{\rho}^{<12>(2)}(z^1,z^2) = -2Kn^2\tilde{g}\Gamma^2_{22}\frac{\partial \tilde{T}^{(0)}}{\partial z^1},\\
&\tilde{\rho}^{<22>(2)}(z^1,z^2) = 2Kn^2\tilde{g}\left[\Gamma^1_{11}\frac{\partial \tilde{T}^{(0)}}{\partial z^1} + \frac{1}{2}\frac{\partial^2 \tilde{T}^{(0)}}{\partial (z^1)^2}\right],\\
&\tilde{\rho}^{<11>(2)}(z^1,z^2) = -2Kn^2\tilde{g}\left[\Gamma^1_{11}\frac{\partial \tilde{T}^{(0)}}{\partial z^1} - \frac{3}{2}\frac{\partial^2 \tilde{T}^{(0)}}{\partial (z^1)^2}\right].
\end{aligned} \tag{46}$$

Whence, by substituting the zeroth-order temperature field $(37)_2$ appropriate the two Poiseuille and Couette flow respectively, it is possible to get explicit solutions. These solutions are shown in Figs.10-13.

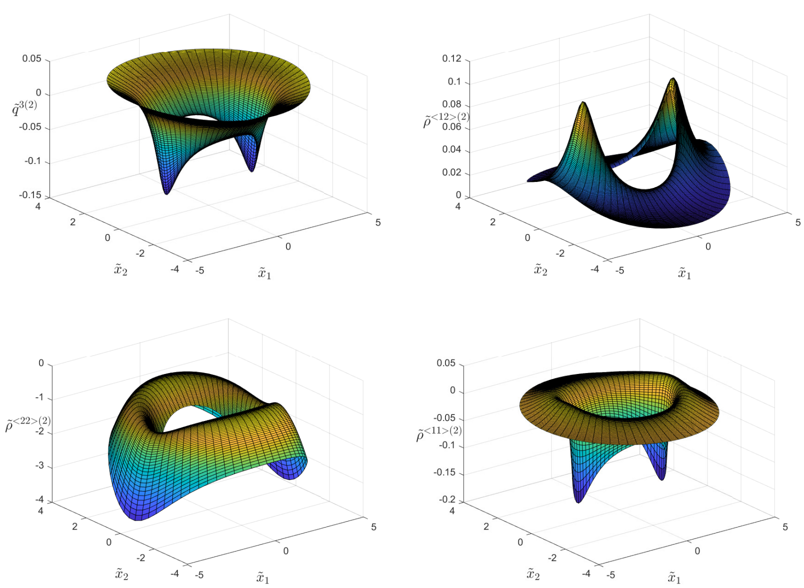

Figure 10: Elliptical coordinates in Poiseuille Problem.

Solutions (46) are the main results of this paper. Indeed, they describe some non-linear effects in addition to the classical Navier-Stokes and Fourier

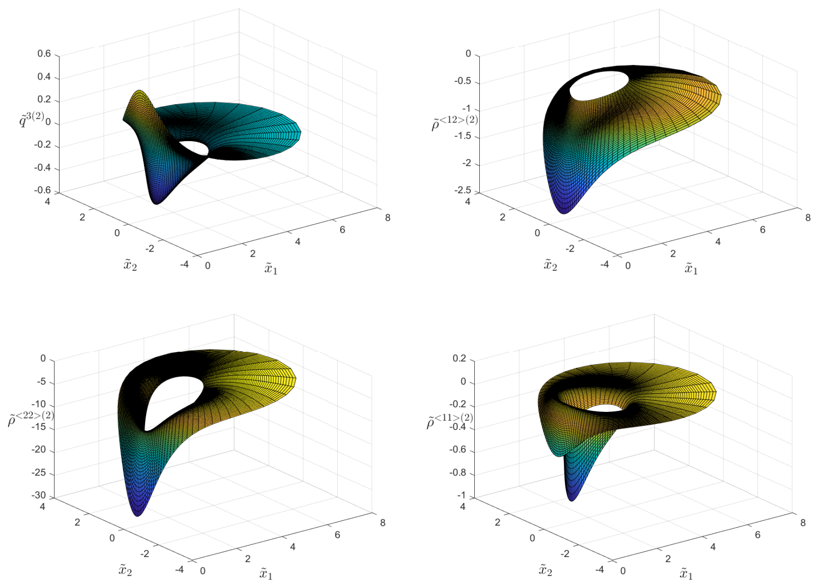

Figure 11: Bi-cylindrical coordinates in Poiseuille Problem.

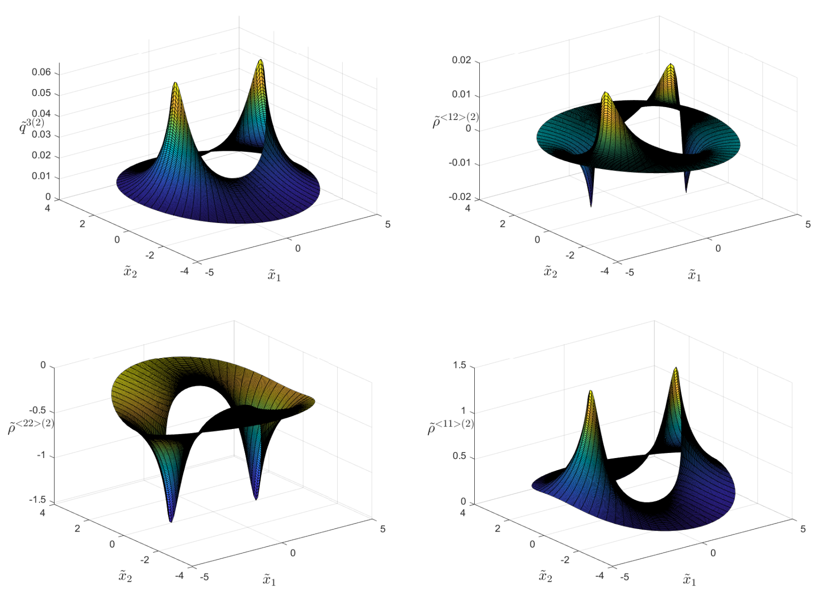

Figure 12: Elliptical coordinates in Couette Problem.

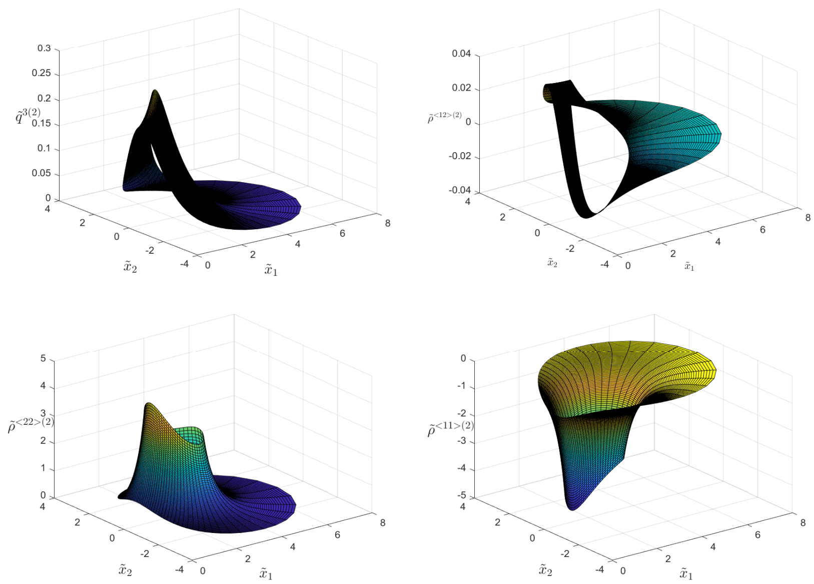

Figure 13: Bi-cylindrical coordinates in Couette Problem.

Laws. In fact, we observe in Figs.10-13 a non-vanishing heat flux component $\tilde{q}^3$ in the direction of the flow, that depends on the velocity and the temperature fields. There exist some non-vanishing components of the traceless part of the stress tensor $\tilde{\rho}^{<11>}$, $\tilde{\rho}^{<22>}$, $\tilde{\rho}^{<12>}$. These contributions are already obtained in the linearized case. Here, in the non-linear case, it is possible to highlight also their dependence on the velocity field.

It could be interesting to get solutions of the complete set of equations (25). A possible way to solve this kind of problems is already under investigation with some numerical method as in [21, 22, 23].

7 Conclusions and final remarks

The stationary heat transfer problem in a rarefied gas is studied together with the Couette and Poiseuille flows. Instead of Classical Thermodynamics, Rational Extended Thermodynamics [31, 36, 37] is used in order to describe such flows. This makes the description of the problem more precise but also more complex.

In order to recover some solutions, firstly the linearized field equations are considered. They are analytically integrated but, due to the linearization, the equations for the temperature and the velocity fields are uncoupled. Furthermore, the temperature and the heat flux coincide with those predicted by the Fourier law and the velocity field coincides with the behavior predicted by the Navier-Stokes case. In the linearized case, only some supplementary components of the stress tensor don't vanish. These components, that depend on the temperature and not on the velocity field, are already put in evidence in [6], where it was shown that the heat conduction causes stresses inside of the gas and these effects are described by some non-vanishing components of the stress tensor.

In order to obtain more accurate results, a perturbation analysis is performed like in [8]. Then, the non-linear effects are emphasized. A new heat flux component in the direction of the flow is observed that depends on the geometry of the problem and on the flow under consideration. This new component is predicted by the kinetic theory, but it cannot be present inside the Classical Thermodynamic theory that assume the heat flux proportional to the temperature gradient. Furthermore, non-vanishing components of the stress tensor are obtained and their dependence on the geometry is presented.

We can conclude once more that the field equations of Rational Extended Thermodynamics are always able to furnish more detailed solutions and more reliable results when the geometry and the flow are more complex, too.

It could be interesting to describe other phenomena and to show other effects in the solutions of Rational Extended Thermodynamics. Furthermore, it would be remarkable to solve numerically the whole set of fields equations (25), at least in some particular cases.

Acknowledgements. Paper written with financial support of Istituto Nazionale di Alta Matematica Francesco Severi (INDAM), GNFM.

References

[1] T. Arima and M.C. Carrisi, Monatomic gas as a singular limit of relativistic theory of 15 moments with non-linear contribution of microscopic energy of molecular internal mode, *Ann. Phys.* 460 (2024), 169576.

[2] T. Arima, M.C. Carrisi, S. Pennisi and T. Ruggeri, Relativistic kinetic theory of polyatomic gases: classical limit of a new hierarchy of

moments and qualitative analysis, *Partial Differ. Equations Appl.* 3 (2022), 39.

[3] E. Barbera and F. Brini, Frame dependence of stationary heat transfer in an inert mixture of ideal gases, *Acta Mech.* 225 (2014), 3285-3307.

[4] E. Barbera and F. Brini, New extended thermodynamics balance equations for an electron gas confined in a metallic body, *Ric. Mat.* 70 (2021), 181-194.

[5] E. Barbera and F. Brini, Non-isothermal axial flow of a rarefied gas between two coaxial cylinders, *Atti Accad. Peloritana Pericolanti Cl. Sci. Fis. Mat. Natur.* 95 (2017), A1.

[6] E. Barbera and F. Brini, On stationary heat conduction in 3D symmetric domains: an application of extended thermodynamics, *Acta Mech.* 215 (2010), 241-260.

[7] E. Barbera and F. Brini, Stationary heat transfer in helicoidal flows of a rarefied gas, *Europhys. Lett.* 120 (2018), 34001.

[8] E. Barbera, F. Brini and G. Valenti, Some non-linear effects of stationary heat conduction in 3D domains through extended thermodynamics, *Europhys. Lett.* 98 (2012), 54004.

[9] E. Barbera and I. Müller, Inherent frame dependence of thermodynamic fields in a gas, *Acta Mech.* 184 (2006), 205-216.

[10] E. Barbera and A. Pollino, A hyperbolic reaction–diffusion model of chronic wasting disease, *Ric. Mat.* 74 (2025), 669-681.

[11] E. Barbera and A. Pollino, A rational extended thermodynamic model for nanofluids, *Fluids* 9 (2024), 193.

[12] E. Barbera and A. Pollino, A three-phase model for blood flow, *Ric. Mat.* 74 (2025), 151-162.

[13] P. Bassanini, C. Cercignani and C.D. Pagani, Comparison of kinetic theory analyses of linearized heat transfer between parallel plates, *Int. J. Heat Mass Transfer* 10 (1967), 447-460.

[14] P.L. Bhatnagar, E.P. Gross and M. Krook, A model for collision processes in gases. I. Small amplitude processes in charged and neutral one-component systems, *Phys. Rev.* 94 (1954), 511.

[15] F. Brini and L. Seccia, Acceleration waves and oscillating gas bubbles modelled by rational extended thermodynamics, *Proc. R. Soc. A* 478 (2022), 20220246.

[16] F. Brini and L. Seccia, Acceleration waves in cylindrical shrinking gas bubbles, *Nucl. Sci. Eng.* 197 (2023), 2301-2316.

[17] F. Brini and L. Seccia, The role of the dynamic pressure in the behavior of an oscillating gas bubble, *Phys. Fluids A* 36 (2024), 097151.

[18] S. Chapman and T.G. Cowling, *The Mathematical Theory of Non-Uniform Gases: An Account of the Kinetic Theory of Viscosity, Thermal Conduction and Diffusion in Gases*, Cambridge, 1990.

[19] G. Consolo, C. Currò, G. Grifò and G. Valenti, Oscillatory periodic pattern dynamics in hyperbolic reaction-advection-diffusion models, *Phys. Rev.* E 105 (2022), 034206.

[20] S.R. De Groot and P. Mazur, *Non-Equilibrium Thermodynamics*, North-Holland, Amsterdam, 1962.

[21] L. Desiderio, S. Falletta, M. Ferrari and L. Scuderi, CVEM-BEM coupling for the simulation of time-domain wave fields scattered by obstacles with complex geometries, *Comput. Methods Appl. Math.* 23 (2023), 353-372.

[22] L. Desiderio, S. Falletta, M. Ferrari and L. Scuderi, CVEM-BEM coupling with decoupled orders for 2D exterior Poisson problems, *J. Sci. Comput.* 92 (2022), 96.

[23] L. Desiderio, S. Falletta, M. Ferrari and L. Scuderi, On the coupling of the curved virtual element method with the one-equation boundary element method for 2D exterior Helmholtz problems *SIAM J. Numer. Anal.* 60 (2022), 2099-2124.

[24] W. Dreyer and H. Struchtrup, Heat pulse experiments revisited, *Cont. Mech. Thermodyn.* 5 (1993), 3-50.

[25] H. Grad, On the kinetic theory of rarefied gases, *Commun. Pure Appl. Math.* 2 (1949), 331-407.

[26] H. Grad, *Principles of the Kinetic Theory of Gases, Thermodynamik der Gase/Thermodynamics of Gases*, Springer, Berlin/Heidelberg, Germany, 1958.

[27] G. Grifò, G. Consolo, C. Currò and G. Valenti, Rhombic and hexagonal pattern formation in 2D hyperbolic reaction–transport systems in the context of dryland ecology, *Phys. D* 449 (2023), 133745.

[28] G.M. Kremer and I. Müller, Thermal Conductivity and dynamic pressure in extended Thermodynamics of chemically reacting mixtures of gases, *Ann. Henri Poincaré* 69 (1998), 309-334.

[29] I.S. Liu, I. Müller and T. Ruggeri, Relativistic thermodynamics of gases, *Annal. Phys.* 169 (1986), 191-219.

[30] I. Müller, *Thermodynamics*, Pitman, London, 1996.

[31] I. Müller and T. Ruggeri, *Rational Extended Thermodynamics* (Vol. 37), Springer Science Business Media, 2013.

[32] I. Müller and T. Ruggeri, Stationary Heat Conduction in Radially Symmetric Situations - An Application of Extended Thermodynamics, *J. Non-Newton. Fluid Mech.* 119 (2004), 139-143.

[33] T. Ohwada, Heat flow and temperature and density distributions in a rarefied gas between parallel plates with different temperatures. Finite-difference analysis of the nonlinear Boltzmann equation for hard-sphere molecules, *Phys. Fluids A* 8 (1996), 2153-2160.

[34] T. Ohwada, Y. Sone and K. Aoki, Numerical analysis of the shear and thermal creep flows of a rarefied gas over a plane wall on the basis of the linearized Boltzmann equation for hard-sphere molecules, *Phys. Fluids A* 1 (1989), 1588-1599.

[35] S. Pennisi and T. Ruggeri, Relativistic extended thermodynamics of rarefied polyatomic gases, *Ann. Phys.* 377 (2017), 414-445.

[36] T. Ruggeri and M. Sugiyama, *Rational Extended Thermodynamics Beyond the Monatomic Gas*, Springer, New York, 2015.

[37] T. Ruggeri and M. Sugiyama, *Classical and Relativistic Rational Extended Thermodynamics of Gases*, Springer, 2021.

[38] H. Struchtrup, An extended moment method in radiative transfer. The matrices of mean absorption and scattering coefficients, *Ann. Phys.* 257 (1997), 111-135.

[39] M. Trovato, Quantum maximum entropy principle and quantum statistics in extended thermodynamics, *Acta Appl. Math.* 132 (2014), 605-619.

[40] M. Trovato, P. Falsaperla and L. Reggiani, Maximum-entropy principle for ac and dc dynamic high-field transport in monolayer graphene, *J. Appl. Phys.* 125 (2019), 174901.

[41] C. Truesdell, The physical components of vectors and tensors, *ZAMM-J. Appl. Math. Mech.* 33 (1953), 345-356.

[42] W. Weiss and I. Müller, Light scattering and extended thermodynamics, *Cont. Mech. Thermodyn.* 7 (1995), 123–177.

[43] W. Weiss, Continuous shock structure in extended thermodynamics, *Phys. Rev. E*, 52 (1995), 5760.

[44] G. Wendt, R.W. King, F.E. Borgnis, C.H. Papas, H. Bremmer, L. Hartshorn, J.A. Saxton and G. Wendt, *Statische Felder und stationäre Ströme.* In: Elektrische Felder und Wellen / Electric Fields and Waves. Handbuch der Physik / Encyclopedia of Physics, vol 4 / 16. Springer, Berlin, Heidelberg.